JOURNAL OF MATERIALS SCIENCE 26 (1991) 3991–3995

Microstructure and phase composition of ZrO_2–CeO_2 thermal barrier coatings

P. D. HARMSWORTH, R. STEVENS
Division of Ceramics, School of Materials, The University of Leeds, Leeds LS2 9JT, UK

The microstructure and phase composition of zirconia plasma-sprayed thermal barrier coatings containing 12 to 25 wt% ceria addition have been investigated. Coatings containing less than 20 wt% CeO_2 are composed of a monoclinic and retained metastable transformable tetragonal phase due to the constraint developed by the small crystal size. This phase transforms readily under moderate thermal stresses. Compositions greater than 20 wt% CeO_2 are composed only of a metastable non-transformable tetragonal, tz′ structure, resistant to transformation under thermal or mechanical stresses. The microstructure of this phase shows microstructural similarities to the high-yttria t′-phase in the ZrO_2–Y_2O_3 system, such as transformation twins and anti-phase boundaries. This suggests that the phase observed in the ZrO_2–CeO_2 system forms by a similar mechanism.

1. Introduction

Zirconia thermal barrier coatings (TBCs) are increasingly being used by aircraft engine manufacturers as a means of improving engine efficiency and service life. Coating compositions giving optimum performance at elevated temperatures were found to have an optimum stabilizer content of around 8 wt % yttria. The microstructure and phase compositions of these coatings have been widely studied. A number of reasons for their improved stability and durability have been identified [1], such as retention of the metastable t′ phase on cooling and a microcracked lamellar microstructure which acts to improve compliance [2] of the ceramic when dimensional changes are to be accommodated.

Recently, considerable interest has turned to replacing yttria with ceria as the stabilizing oxide added to zirconia ceramics and coatings [3]. The reasons for this change are economic, to reduce production costs, as yttria is considerably more expensive than ceria. This is especially the case for coatings which require a higher proportion of stabilizing oxide than conventional zirconia ceramics. Secondly, it has been shown [4] that Ce-TZP ceramics can attain significantly greater toughness than Y-TZP ceramics. This has been found to be an important parameter determining properties and performance in TBCs [2], and would suggest that coatings based upon the ZrO_2–CeO_2 system should have a potentially superior thermal shock resistance to those based on the ZrO_2–Y_2O_3 system. This would result in improved performance and extended thermal cycle life.

2. Experimental procedure

A range of ZrO_2–CeO_2 coatings containing 12, 15, 20 and 25 wt % CeO_2 were plasma-sprayed at Rolls Royce, Derby. These were then characterized by SEM, TEM and XRD to investigate the microstructure and phase composition of the coatings. The results were then compared with the latest phase diagrams, and related to previous experience with coatings based on the ZrO_2–Y_2O_3 system [2].

3. Results and discussion

3.1. Microstructure

Microstructural examination of the fracture surfaces, using scanning electron microscopy (Fig. 1), showed the coatings to have a similar lamellar microstructure to those of the ZrO_2–Y_2O_3 system [1], characteristic of the layered structure formed by the plasma-spraying process. The individual lamellae were somewhat thinner, typically 1–2 μm thick. This reduced thickness of the lamellae is likely to be a result of either a greater impact velocity or a reduction in the viscosity of the molten ceramic at the time of impact. The columnar grain size was also smaller, reflecting an

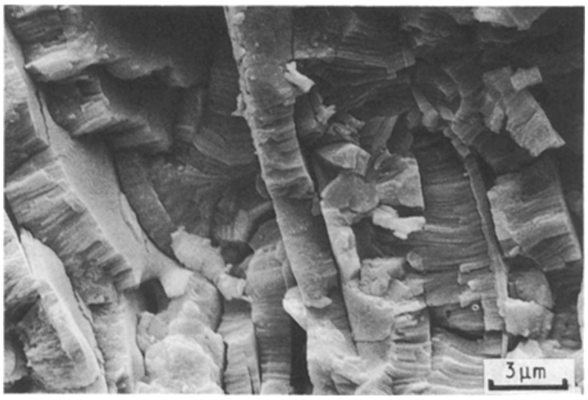

Figure 1 SEM fracture surface of a ZrO_2–CeO_2 coating, illustrating the thin lamellae and fine, well-delineated columnar grain structure.

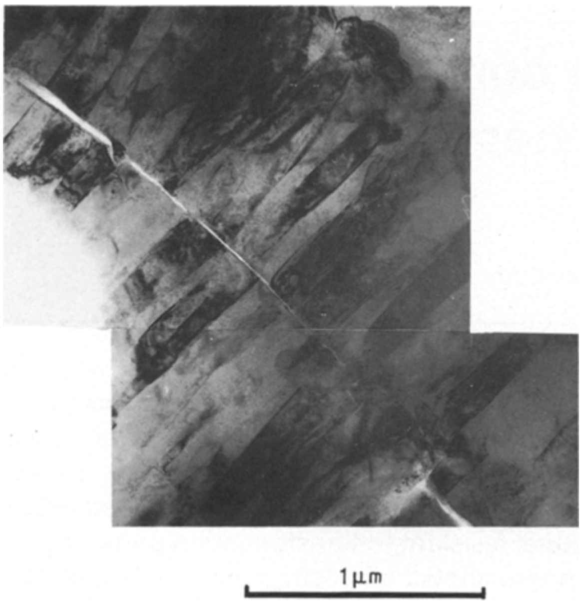

Figure 2 TEM showing the lamellar structure in the ZrO_2–CeO_2 coating. The composition is 12 wt % CeO_2.

increased number of nucleation sites promoted by extended splat spread.

TEM analysis of the lamellar structure within the coating (Fig. 2) also showed a finer columnar grain structure in the lamellae, the grains being typically 0.1 µm × 1 µm. Fig. 2 also shows a similar interlamellar porosity to that observed in the ZrO_2–Y_2O_3 system [1]. Fig. 3 shows a TEM section parallel to the substrate surface; intergranular microcracking can be seen to occur along the boundaries of the fine grains. This may well have been initiated by transformation of the retained tetragonal phase to monoclinic symmetry, the crack propagating along a weak grain-boundary glassy phase.

3.2. Phase analysis

X-ray diffraction (XRD) analysis at low angles, in the range 27–32°, and high angles in the range 72–76°, was used to investigate the amount of monoclinic, tetragonal and cubic phases present in the coatings.

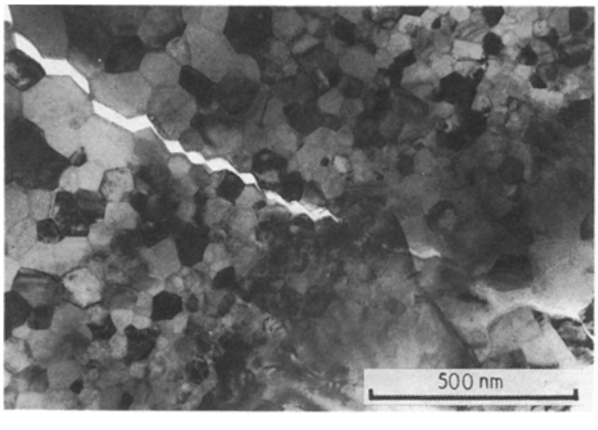

Figure 3 TEM showing grain-boundary microcracking and separation of the fine grains in a ZrO_2–20 wt % CeO_2 coating.

The results of standard low-angle XRD analysis between the cycles of 27–30° of the $(1\,1\,1)_m$ and $(1\,1\,1)_{c/t}$ peaks, and also the volume percentage of monoclinic phase, V_m, estimated from the integrated intensities of the peaks, are shown in Table I. A decrease in the amount of m-ZrO_2 from 20% to zero was found with increasing CeO_2 addition. However, the amount of monoclinic phase present is significantly less in all samples than is predicted by any of the published phase diagrams (Fig. 4).

The coatings were subsequently analysed between the 2θ angles of 72–76° to attempt to determine the cubic and tetragonal phase contents. For all the compositions examined, only two peaks could be identified in this region, corresponding to the $(4\,0\,0)_t$ and $(0\,0\,4)_t$ peaks. No evidence for the $(4\,0\,0)_c$ peak, which is expected to be present in these compositions, was found in any of the coatings investigated. The lattice parameters, peak separation $\Delta 2\theta_t$ and c/a ratio for the tetragonal peaks for each composition are shown in Table II.

It can be seen in Table II that there is a gradual decrease in the tetragonal peak separation $\Delta 2\theta_t$ and that the c/a ratio decreases with increasing CeO_2 addition. A plot of the c_t and a_t lattice parameters (Fig. 5) showed a linear increase in both parameters with increasing ceria content. The slope of the a lattice parameter was found to be greater than that of c_t, and

TABLE I Low-angle XRD peaks from ZrO_2–CeO_2

Composition	2θ (deg)			
	$(1\,1\,1)_m$	$(1\,1\,1)_m$	$(1\,1\,1)_{c/t}$	V_m (%)
12Ce	31.4	28.25	30.3	20.2
15Ce	31.35	28.3	30.2	8.4
20Ce	31.4	28.3	30.2	7.35
25Ce	31.25	28.3	30.0	0

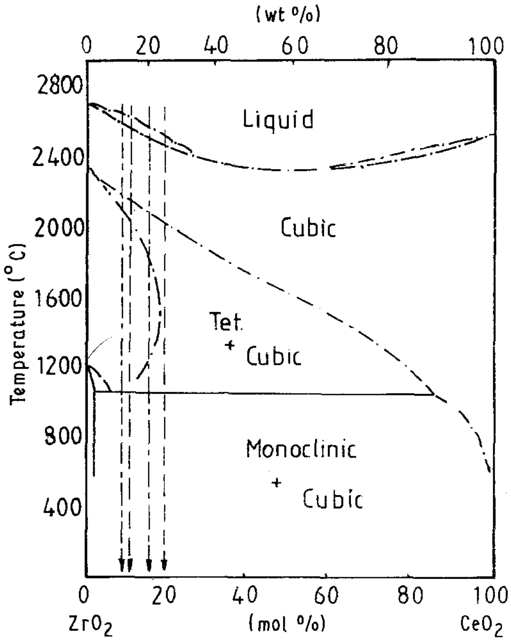

Figure 4 Phase diagram of the ZrO_2–CeO_2 system according to Tani *et al.* [6], showing the compositions investigated.

TABLE II High-angle XRD of ZrO_2–CeO_2

Composition	a_t (nm)	c_t (nm)	$\Delta 2\theta_t$	c_t/a_t
12Ce	0.51	0.5192	1.35	1.0176
15Ce	0.5116	0.5192	1.25	1.0149
20Ce	0.512	0.5196	1.2	1.0141
25Ce	0.514	0.52	0.95	1.0117

it is the change in this parameter that caused most of the change in the *c/a* ratio.

The limited number of previous studies on the ZrO_2–CeO_2 system makes comparison with the present results difficult. Much of the early work on the phase diagram for this system gave rise to conflicting results, often a consequence of the lengthy periods required to reach equilibrium. The latest phase diagram has been produced by Yoshimura *et al.* [5, 6] using hydrothermal techniques, which were found to accelerate the transformations and hence provide more accurate results at temperatures below 1500 °C.

A comparison of the monoclinic phase content present in the coating with that predicted from the phase diagrams of Yoshimura *et al.* [6] and of others [7] has shown that the as-sprayed coatings contain less m-ZrO_2 than expected. XRD analysis at high angles showed the remainder of the coatings to be composed of a retained tetragonal phase with no evidence for c-ZrO_2. Both a_t and c_t, the tetragonal lattice parameters, were found to increase with ceria content. Such an increase in the tetragonal lattice parameters has also been detected by Duez and Odell [7], who suggested the increase to be due to the replacement of zirconium ions (ionic diameter 0.174 nm) by cerium ions (ionic diameter 0.204 nm).

In the present study, however, a decrease in the *c/a* ratio from 1.0175 to 1.0117 in the 12 and 25 wt% CeO_2 coatings, respectively, was observed, which was not reported by Duez and Odell [7]. Only the higher value for the 12 wt % CeO_2 agrees with the equilibrium *c/a* ratio as measured in the previous studies [7]. Yoshimura *et al.* [5] measured an average *c/a* ratio for an equilibrium solid solution of tetragonal phase containing 23 wt% (18 mol %) CeO_2 to be 1.0172, and Duez and Odell [7] found the tetragonal phase in a rapidly cooled 20 wt % CeO_2 sample to have a *c/a* ratio of 1.015. Neither of these studies reported a gradual reduction in the *c/a* ratio with increasing CeO_2 content.

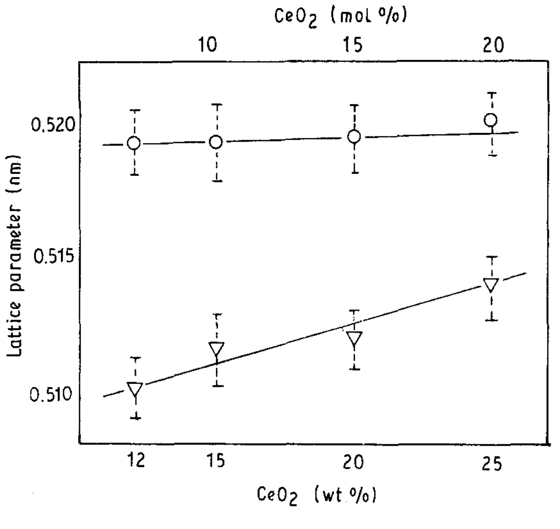

Figure 5 Lattice parameters (○) c_t and (▽) a_t versus composition for the tetragonal phase in the ZrO_2–CeO_2 coatings.

A further significant difference between the phase compositions of the coatings and the phase diagrams of both Duez and Odell [7] and Yoshimura *et al.* [5] was the lack of any c-ZrO_2 in the as-sprayed structure. Duez and Odell suggested that a two-phase (c + t) ZrO_2 composition should be stable at room temperature. However, the work of Yoshimura and coworkers [5, 6], which is probably more accurate in the low temperature range, indicated that only the monoclinic and cubic ZrO_2 solid solutions were stable at room temperature, the tetragonal eutectoid existing at 1100 °C.

3.3. Stability of coatings

XRD results on the as-sprayed coatings indicated that the plasma-spraying of ZrO_2–CeO_2 gave rise to the formation of a tetragonal phase, not reported in the most recent phase diagrams. The *c/a* ratio of this phase was found to approximate to the high-temperature equilibrium tetragonal phase in the low CeO_2 compositions ($< 20\%$ CeO_2), but was significantly smaller in the higher CeO_2 compositions. The ZrO_2–Y_2O_3 system has shown us that rapid quenching of the compositions 6–12 wt % Y_2O_3 induced by plasma spraying resulted in the displacive transformation, giving rise to a high Y_2O_3 non-transformable t′ phase with a much smaller *c/a* ratio than the equilibrium transformable tetragonal phase [8].

To investigate whether the tetragonal phase formed in the ceria coatings was either a transformable or a non-transformable tetragonal phase (t′ phase), the stability of the coatings with regard to the t–m transformation was tested. This was determined both by grinding and by rapid thermal cycling between 900 and 20 °C, i.e. above and below the M_s temperature. This procedure was found [9] sufficiently harsh to induce the t–m transformation of retained tetragonal particles, due to the thermal expansion hysteresis developed during the martensitic transformation to m-ZrO_2:

1. Grinding for up to 5 min in a pestle and mortar showed no significant increase in the amount of monoclinic zirconia in any composition.
2. Thermal cycling resulted in significant changes in the phase composition of the low-ceria coatings after just one thermal cycle (Table III).

It is apparent that the thermomechanical stress induced within the material during thermal cycling is sufficient to disrupt the matrix constraint, resulting in a permanent transformation of the tetragonal phase to monoclinic [10]. The time for which the samples were held at 900 °C was not sufficient to allow significant diffusion and thus to cause transformation of a metastable non-transformable t′-ZrO_2 phase.

Significant transformation was observed in coatings containing 12–20 wt % ceria, exposing the lack of

TABLE III Monoclinic phase content (vol %) after thermal cycling

Composition	Number of cycles 900 → 20 °C		
	0	1	8
12Ce	20.2	61.8	73.3
15Ce	8.4	34.2	40.8
20Ce	7.35	26.0	26.6
25Ce	0	3.1	2.7
SCY6	4		5.8
SCY8	1.6		1.5

stability of the tetragonal phase in these low ceria compositions. The coatings can be observed in Fig. 6 to have undergone extensive cracking during the thermal cycling arising from the volume expansion which occurs on transformation. Using high-angle XRD, the remainder of the untransformed material in the coatings was observed to have tetragonal symmetry. This tetragonal phase in the coatings, which contained greater than 20 wt % ceria, was found to have a high stability, similar to that of ZrO_2 coatings containing greater than 6 wt % Y_2O_3 [1, 2].

3.4. General discussion of results

The XRD data and thermal cycling experiments have revealed a number of similarities between the tetragonal phases in the ZrO_2–CeO_2 and ZrO_2–Y_2O_3 systems. These similarities are not surprising considering the similar shape of their respective phase diagrams. Plasma-sprayed coatings containing less than 20 wt % ceria will pass through the tetragonal single-phase field on cooling from the spray temperature, forming a single tetragonal-phase solid solution in the coating.

The small grain size characteristic of the plasma-sprayed zirconia body is below that required for spontaneous transformation to m-ZrO_2, causing the tetragonal phase to be retained to room temperature [11, 12]. Even the removal of matrix constraint by harsh means, such as by grinding, was insufficient to induce the transformation. The lattice parameters for the tetragonal phase in these coatings was similar to those measured by Yoshimura *et al.* [5] and Duez and Odell [7] on fully dense sintered and aged material, indicating that a similar tetragonal structure had been formed. Thermal cycling was, however, found to induce sufficient stress on the grains to initiate the stress-induced martensitic transformation. The amount of m-ZrO_2 formed was still below that suggested by the phase diagram [6] and increasingly so with further stabilizer additions, the balance of the coating retaining tetragonal symmetry.

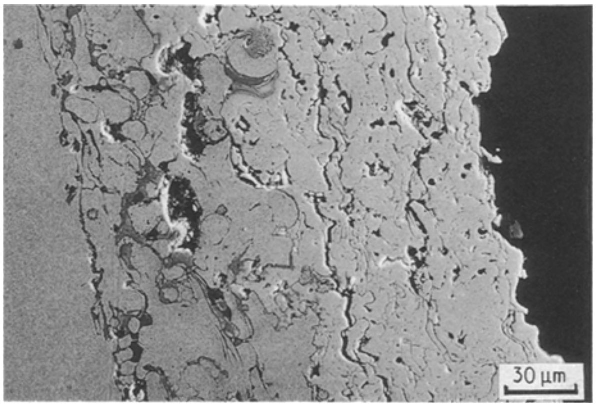

Figure 6 SEM showing increased microcracking in ZrO_2–15 wt% CeO_2 after thermal cycling. Note the convoluted nature of the cracking, which follows the interfaces of the deposition layers.

Compositions containing greater than 20 wt % ceria were also observed to have t-symmetry; however, they did not transform during thermal cycling. These compositions passed through the two-phase (t + c) region of the phase diagram (Fig. 4) such that on cooling the two-phase structure was formed. The transformation conditions are therefore considered to be suitable to induce a similar c → t′ transformation to that in the ZrO_2 system containing 6–12 wt % Y_2O_3. This gives rise to the formation of a non-transformable high-CeO_2 structure of tetragonal symmetry similar to the t′ phase observed in the ZrO_2–Y_2O_3 system.

The reduced peak separation Δd and low c/a ratio of this tetragonal phase supports the similarity between it and the t′-ZrO_2. Also, the lack of any cubic phase, despite having passed through the (t + c) two-phase field, suggests a preference for the displacive transformation and retention of a t′-like structure during plasma spraying. This is not entirely surprising in view of the time and temperature that would be required to allow the necessary diffusion of Ce^{4+} to equilibrate the cubic and tetragonal phases.

The existence of a metastable ceria-rich tetragonal phase in quenched samples containing between 20 and 60 wt %, ceria, which have undergone a non-equilibrium cooling rate, has been observed by Meriani [13]. This author noted a splitting of the cubic fluorite peak in samples below 55 mol % CeO_2. The splitting was found to increase with increased firing temperature. The *d*-spacings were also found to be larger than those found for the equilibrium tetragonal solid solution, indicating the formation of a new metastable tetragonal phase with a high ceria concentration and named tz′. Short heat treatments below 1450 °C were found to restore the expected equilibrium t and c phases. The microstructure of this tz′ phase was observed by SEM to exhibit twinned colonies, thought to develop during a diffusionless type of transformation.

3.5. TEM analysis

In order to examine this tz′-CeO_2 phase further and compare it with previous studies of t′-Y_2O_3 in coatings [2], TEM samples were prepared. Although the grain size is much smaller, individual larger grains of up to 1 µm revealed the metastable tz′ phase in ZrO_2–CeO_2 to have a very similar structure to the t′ phase in ZrO_2–Y_2O_3 (Fig. 7). The grains can be observed to be twinned as described by Meriani [13]. There is also evidence of a domain-like structure having the contrast typical of antiphase boundaries (APBs). Microstructural features such as these were shown to be characteristic of the displacive c–t′ transformation in the yttria system [14]. They therefore

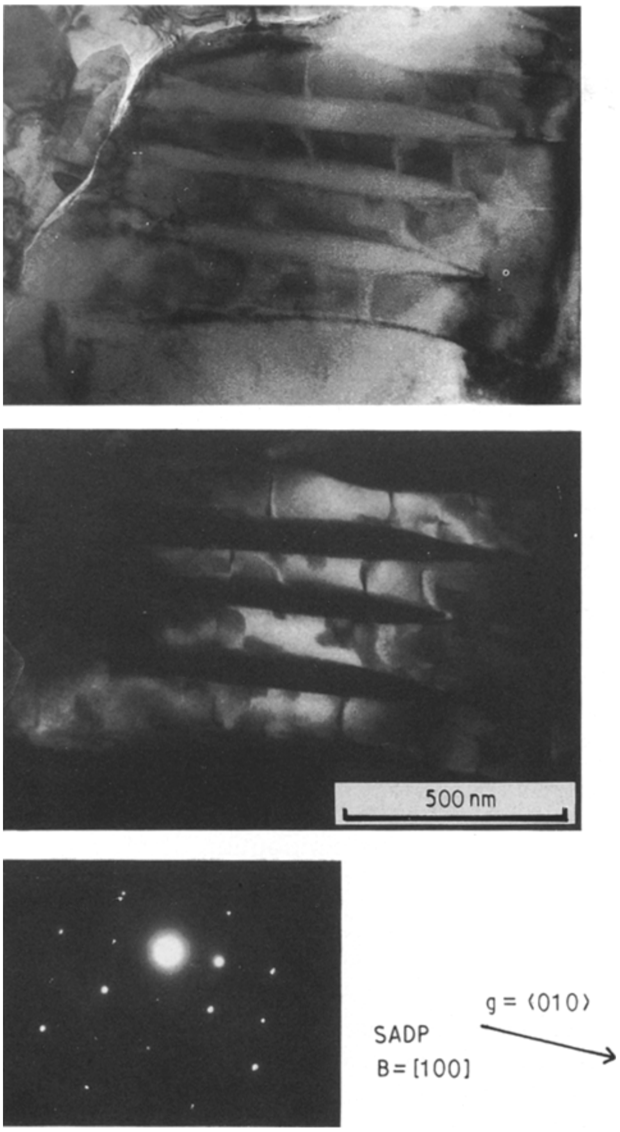

Figure 7 TEM showing the tz′ structure in ZrO_2–25 wt % CeO_2; the grains are twinned and contain APBs which are clearly apparent in both the bright-field and dark-field micrographs.

suggest that the CeO_2-rich metastable tz′ phase in the zirconia–ceria system forms from the cubic by a similar mechanism. Recent studies have observed similar features, although as yet this phase has not been characterized to the same extent as t′-ZrO_2–Y_2O_3.

4. Conclusions

A number of important conclusions can be drawn from an analogy with coatings in the yttria system. Firstly, coatings containing less than ~ 20 wt % CeO_2 are composed primarily of the monoclinic and the retained transformable tetragonal phase. A large proportion of this t-phase is susceptible to transformation to m-ZrO_2 after short-term thermal cycling at moderate temperatures. The volume expansion and shear strains associated with transformation give rise to increased cracking of the coating, reducing the thermal protection and increasing coating diffusivity and bond coat oxidation. This is likely to make the low-CeO_2 compositions unsuitable for high-temperature TBC applications.

Coatings containing greater than 20 wt % CeO_2 are composed of a new metastable tetragonal non-transformable tz′-like structure which is resistant to transformation by grinding or by thermal cycling to moderate temperatures. This phase shows a number of microstructural similarities to the t′ phase, and is likely to form by a similar mechanism to the t′ phase in the ZrO_2–Y_2O_3 system. The improved stability of this phase, and an analogy with the optimum yttria compositions, suggests that these ceria compositions are more suitable for coating applications. Significant further work will be required on a far wider range of ceria additions to optimize the ceria content and the consequent phase composition of the coating in order to optimize service life.

Acknowledgements

P.D.H. acknowledges the support of SERC and Rolls Royce during the course of this work. The help of Dr P. Morrell in providing the plasma-sprayed specimens was greatly appreciated.

References

1. P. D. HARMSWORTH and R. STEVENS, *J. Mater. Sci.* in press.
2. *Idem.*, *ibid.* in press.
3. G. W. HEINTZE and R. McPHERSON, in Proceedings of Conference on Surface Coating Technology (1987).
4. T. COYLE, W. COBLENZ and B. A. BENDER, *Amer. Ceram. Soc. Bull.* **62** (1983) 966.
5. M. YOSHIMURA, E. TANI and S. SOMIYA, *Solid State Ionics* **314** (1981) 447.
6. E. TANI, M. YOSHIMURA and S. SOMIYA, *J. Amer. Ceram. Soc.* **66** (1983) 506.
7. P. DUEZ and F. ODELL, *ibid.* **33** (1950) 274.
8. R. A. MILLER, *Adv. Ceram.* **3** (1981) 241.
9. M. WATANABE, S. IIO and I. FAKAURA, *ibid.* **12** (1984) 382.
10. K. TSAKUMA, Y. KUBOTU and T. TSAKIDATE, *ibid.* **12** (1984) 391.
11. T. K. GUPTA, J. H. BECHTOLD, R. C. KANICKI, L. H. CADOFF and B. R. ROSSING, *J. Mater. Sci.* **12** (1977) 2421.
12. T. K. GUPTA and C. A. ANDERSON, *Ceram. Eng. Sci. Proc.* **7** (1986) 1150.
13. S. MERIANI, *Sci. Ceram.* **13** (1986) 1.
14. V. LANTERI, A. H. HEUER and T. E. MITCHELL, *Adv. Ceram.* **12** (1984) 118.

Received 11 October
and accepted 19 October 1990